




WILEY

## RESEARCH ARTICLE

# Anticancer and antileishmanial in vitro activity of gold(I) complexes with 1,3,4-oxadiazole-2(3H)-thione ligands derived from $\delta$ -D-gluconolactone

Andrés Villaseñor Espinosa<sup>1</sup> | Danilo de Souza Costa<sup>1</sup> | Luiza Guimarães Tunes<sup>2</sup> | Rubens L. do Monte-Neto<sup>2</sup>  | Richard Michael Grazul<sup>1</sup> | Mauro Vieira de Almeida<sup>1</sup> | Heveline Silva<sup>3</sup> 

<sup>1</sup>Departamento de Química, ICE, Universidade Federal de Juiz de Fora, Juiz de Fora, MG, Brazil

<sup>2</sup>Instituto René Rachou-Fiocruz Minas, Belo Horizonte, MG, Brazil

<sup>3</sup>Departamento de Química, ICEx, Universidade Federal de Minas Gerais, Belo Horizonte, MG, Brazil

## Correspondence

Heveline Silva, Departamento de Química, ICEx, Universidade Federal de Minas Gerais, 31270-901, Belo Horizonte, MG, Brazil.

Email: hevelinesilva@ufmg.br

## Funding information

Fundação de Amparo à Pesquisa do Estado de Minas Gerais, Grant/Award Number: APQ-03059-16; Universidade Federal de Juiz de Fora; Conselho Nacional de Desenvolvimento Científico e Tecnológico; Coordenação de Aperfeiçoamento de Pessoal de Nível Superior, Grant/Award Number: 88881.133591/2016-01

## Abstract

Four gold(I) complexes conceived as anticancer agents were synthesized by reacting [Au(PEt<sub>3</sub>)Cl] and [Au(PPh<sub>3</sub>)Cl] with ligands derived from  $\delta$ -D-gluconolactone. The ligands' structure was designed to combine desired biological properties previously reported for each group. Ligands were synthesized from  $\delta$ -D-gluconolactone via ketal protection and hydrazide formation followed by cyclization with CS<sub>2</sub> to produce the novel oxadiazolidine-2-thione **7** and **8**. Increasing of the ligands' lipophilicity via ketal protection proved useful since all four gold(I) complexes showed anticancer and antileishmanial properties. The IC<sub>50</sub> values are at low micromolar range, varying from 2 to 3  $\mu$ M for the most active compounds. The free D-gluconate 1,3,4 oxadiazole-derived ligands were neither toxic nor presented anticancer or antileishmanial properties. Triethylphosphine-derived compounds **9** and **10** were more selective against B16-F10 melanoma cell line. Although similar in vitro antileishmanial activity was observed for the gold(I) precursors themselves and their derived complexes, the latter were three times less toxic for human THP-1 macrophage cell line; this result is attributed to an isomeric variation of the D-gluconate ligand and the oxadiazole portion, which was one of the key concepts behind this work. These findings should encourage further research on gold(I) complexes to develop novel compounds with potential application in cancer and leishmaniasis chemotherapy.

## KEYWORDS

antitumor, leishmania, metal, synthesis

## 1 | INTRODUCTION

Gold(I) complexes with saccharide-based ligands have been extensively studied in recent years, as they have shown significant in vitro cytotoxic activity against many cisplatin-resistant tumor cell lines (Rigobello et al., 2008). Unlike cisplatin, which targets DNA to exert its cytotoxic effect, gold(I) complexes interrupt intracellular protein signaling mechanisms (particularly thioredoxin reductase), leading to cell apoptosis

(da Silva Maia, Deflon, & Abram, 2014). The structure of ligands used to synthesize gold(I) complexes has great influence on their biological activity (Yeo et al., 2013). An important factor is the lipophilicity of the ligand, which directly impacts the ability of the complex to penetrate through cell membranes. The insertion of a tertiary phosphine group in some gold(I) complexes (as in auranofin) has consistently resulted in increased biological activity, when compared to their analogous non-phosphorated compounds (Ott et al., 2009).

Despite the myriad ligand possibilities available for gold(I)-based metallodrug synthesis, 1,3,4-oxadiazoles have become an important motif of interest for the design of new drugs due to a plethora of biological properties they possess, including anti-inflammatory, anticancer, antimalarial, antibacterial, anticonvulsant, cytotoxic, tyrosinase inhibitory, angiogenesis inhibitory, hypoglycemic, analgesic, antitubercular, antiemetic, anti-allergic, hypoglycemic, antiedema, antifungal, diuretic, antihypertensive, and antiviral (Leite de Oliveira et al., 2012; Patel et al., 2014). Oxadiazolidine-derived compounds belong to a broader group of heterocyclic molecules, particularly because of their anticancer activity (Chaves et al., 2014). This makes them very appealing for use in the synthesis of ligands. The intrinsic properties of these ligands could favor in vivo performance by promoting a combinatory effect of different biological activities. The significance of this work lies in the design and synthesis of novel ligands using multiple biologically active groups in order to enhance the overall effectivity and selectivity of the gold(I) complexes. Our research group already reported several studies describing gold(I) complexes with different ligands based on different substrates, such as benzyl and benzoyl chloride (Chaves et al., 2014), alcohols and fatty acids (de Almeida et al., 2017), some monosaccharides (Chaves et al., 2015), and adamantane (Garcia et al., 2016); all of them showed selective cytotoxicity against tumor-derived cell lines and were more effective than cisplatin. Some of these compounds also presented antileishmanial activity against *Leishmania infantum* and *Leishmania braziliensis* intracellular amastigotes and axenic promastigotes (Chaves et al., 2016). These *Leishmania* species are, respectively, the main etiological agents of visceral and cutaneous leishmaniasis in Brazil (Falcão et al., 2016). Leishmaniasis is a worldwide neglected disease and a public health problem that urgently requires new alternative chemotherapeutic agents for control and disease eradication. Curiously enough, parasitic infections, including those caused by *Leishmania* parasites, present some similarities with cancer (Oliveira, 2014). Both *Leishmania* and tumor cells present an elevated cell division rate that cannot be controlled by the host; their energetic metabolism heavily relies on glycolysis; they device strategies to evade the immune system and have multifactorial drug resistance mechanisms. For instance, Miltefosine—originally designed as an antitumoral drug—was repurposed and it is currently the only available oral antileishmanial agent to treat leishmaniasis (Sundar et al., 2002). Recently, adamantane-gold(I) complexes were reported as an oral drug candidate to treat leishmaniasis (Tunes et al., 2020). Gold(I)-based auranofin, which also shows anticancer activity, has also been reported as an effective antileishmanial agent both in vitro and in vivo (Sharlow et al., 2014). These facts justify

continuous and concomitant research for anticancer and antileishmanial agents, which is the main premise behind this work's innovative scheme.

In this work, we explored the use of D-gluconate carbohydrate residues along with 1,3,4-oxadiazoles as ligands. They presented remarkably low toxicity, and the extent of their biological activity was readily distinguishable from that of other ligands (Yoshida et al., 1999). These findings from previous research on ligand structure–activity relations led us to synthesize, characterize, and evaluate the anticancer and antileishmanial activities of two novel ligands and four novel gold(I) complexes, which are described in this work.

## 2 | METHODS AND MATERIALS

### 2.1 | Reagents and instrumentation

All reagents and solvents were used without further purification. [Au(PEt<sub>3</sub>)Cl] is commercially available, and [Au(PPh<sub>3</sub>)Cl] was synthesized from K[AuCl<sub>4</sub>] according to the literature (Baenziger, Bennett, & Soborofe, 1976). Flash chromatography was performed on silica gel (Merck, 70–230 mesh) as the stationary phase. All reactions were monitored by TLC. IR spectra were acquired on a Perkin-Elmer 1720 FTIR spectrometer in the region of 4000–400 cm<sup>-1</sup> as KBr pellets. <sup>1</sup>H NMR (500 MHz), <sup>13</sup>C NMR (125 MHz), and <sup>31</sup>P NMR (202 MHz) spectra were recorded as solutions in CDCl<sub>3</sub> or DMSO-*d*<sub>6</sub> in an Avance III HD BRUKER 500 MHz spectrometer. Chemical shifts were expressed in ppm. All NMR data were reported using the following syntaxes: chemical shift, multiplicity, and integration, followed by coupling constant values. High-resolution mass spectra were recorded on a Shimadzu Biotech-Axima Performance mass spectrometer using laser desorption ionization (LDI) with a time-of-flight (TOF) mass analyzer.

### 2.2 | Synthesis

Figure 1 shows the general synthetic route used in this work.

#### 2.2.1 | Synthesis of compounds 3 and 4

δ-D-gluconolactone was used as the precursor to prepare the isopropylidene compounds **3** and **4**, according to methodology previously described in the literature (Regeling, de Rouville, & Chittenden, 1987). In a 25 ml round-bottom flask, 10 mmol of δ-D-gluconolactone was dissolved in 10 ml of acetone and 3 ml of methanol, followed by addition of 4 ml of 2,2-dimethoxypropane and 50 mg of *p*-toluenesulfonic acid and 50 μl of concentrated H<sub>2</sub>SO<sub>4</sub> as catalysts.

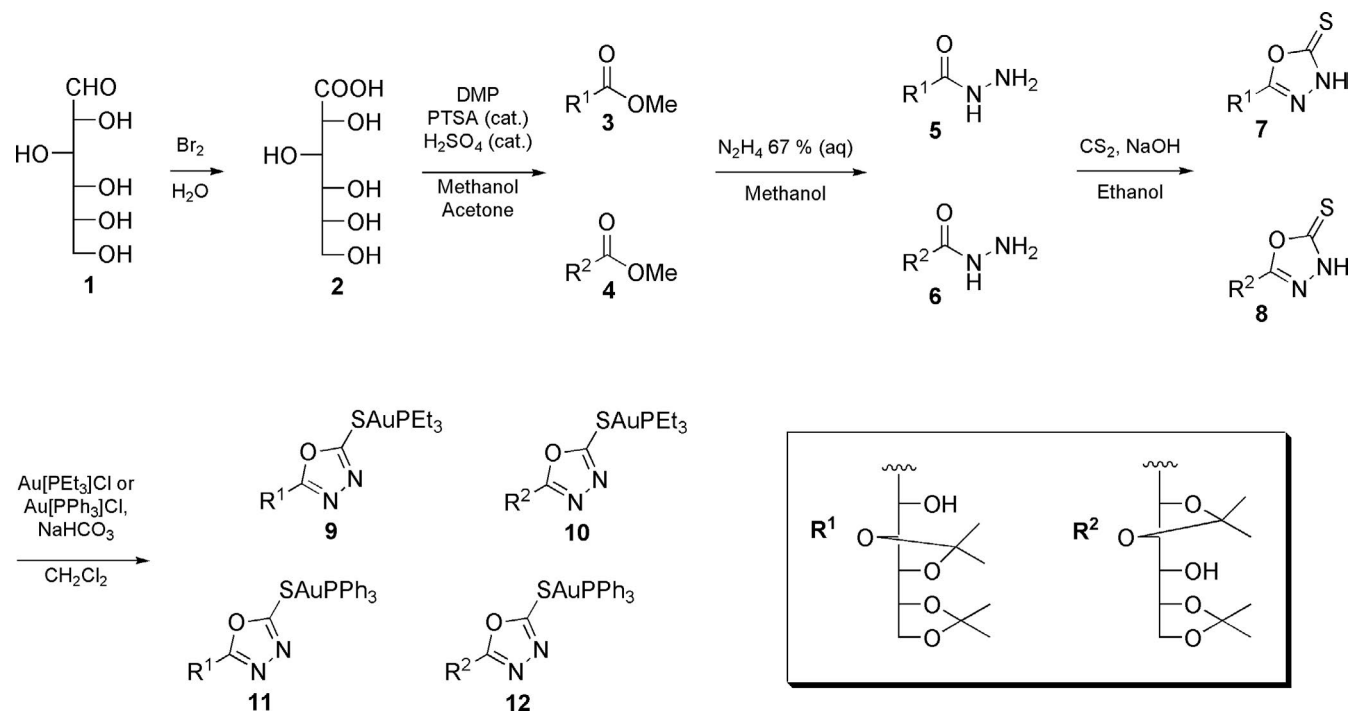


**FIGURE 1** Scheme representing the synthetic route to obtain gold(I) complexes 9–12

The reaction mixture was then stirred for 48 hr at room temperature. Residual acid was removed by liquid–liquid extraction (dichloromethane and brine), and the isomers **3** and **4** were separated by column chromatography. Methyl (3,4)/(5,6)-di-*O*-isopropylidene-D-gluconate **3** and its isomer methyl (2,3)/(5,6)-di-*O*-isopropylidene-D-gluconate **4** were obtained in yields of 44 and 22%, respectively. Their spectral data were in accordance with those reported in the literature (Regeling et al., 1987).

### 2.2.2 | Synthesis of hydrazides 5 and 6

In a 10 ml round-bottom flask, 200 mg of the corresponding starting material was dissolved in 3 ml of methanol and then 200  $\mu\text{L}$  of 67% aqueous hydrazine solution was added. The mixture was stirred for 8 hr at room temperature. Excess hydrazine was removed by liquid–liquid extraction using dichloromethane and brine. The organic phase was evaporated under reduced pressure to yield the desired hydrazides **5** and **6** in quantitative yield.

Hydrazide **5**: oil,  $\mu$ : 68.95 mPa s,  $\rho$ : 1.341  $\text{g}/\text{cm}^3$ , IR (KBr)  $\nu(\text{cm}^{-1})$ : 3500–3300 (O–H stretch), 3,346 and 3,315 (s,  $\text{NH}_2$  asymmetric stretch), 2,985 and 2,917 (m,  $\text{CH}_{\text{aliphatic}}$  asymmetric/symmetric stretch), 1,652 (s, C=O stretch), 1,610 (m,  $\text{NH}_2$  scissoring), 1,518 (m,  $\text{NH}_2$  bending), 1,250, 1,210, 1,170, 1,140, 1,085 (m, s, ketal C–C stretch).  $^1\text{H}$  NMR (500 MHz,  $\text{CDCl}_3$ )  $\delta$  (ppm): 8.84 (s, 1H), 5.60 (d, 1H,  $J = 6.9$ ), 4.27 (s, 1H), 4.22 (dd, 1H,  $J = 7.7$  Hz,  $J = 1.8$  Hz), 4.10 (ddd, 1H,  $J = 7.4$  Hz,  $J = 6.3$  Hz,  $J = 4.7$  Hz), 4.05 (d, 1H,  $J = 8.3$  Hz,

$J = 6.3$  Hz), 3.99 (dd, 1H,  $J = 6.8$  Hz,  $J = 1.7$  Hz), 3.93 (t, 1H,  $J = 7.6$ ), 3.81 (dd, 1H,  $J = 8.3$  Hz,  $J = 4.7$  Hz), 1.33 (s, 3H), 1.31 (s, 3H), 1.27 (s, 3H), 1.26 (s, 3H).  $^{13}\text{C}$  NMR (125 MHz,  $\text{CDCl}_3$ )  $\delta$  (ppm): 170.0, 108.8, 108.7, 80.0, 76.4, 75.8, 69.5, 66.4, 27.0, 26.6, 26.4, 25.0. HRMS (LDI/TOF)  $m/z$   $[\text{M} + \text{H}]^+$  calc.: 291.1556 found: 291.1039.

Hydrazide **6**: oil,  $\mu$ : 62.16 mPa s,  $\rho$ : 1.284  $\text{g}/\text{cm}^3$ , IR (KBr)  $\nu(\text{cm}^{-1})$ : 3,500–3,300 (O–H stretch), 3,330 (s,  $\text{NH}_2$  asymmetric stretch), 2,988 and 2,937 (m,  $\text{CH}_{\text{aliphatic}}$  asymmetric/symmetric stretch), 1,661 (s, C=O stretch), 1,511 (m,  $\text{NH}_2$  bending), 1,270, 1,205, 1,070 (s, ketal C–C stretch).  $^1\text{H}$  NMR (500 MHz,  $\text{CDCl}_3$ )  $\delta$  (ppm): 8.03 (s, 1H), 4.48 (d, 1H,  $J = 8.2$  Hz), 4.21 (dd, 1H,  $J = 8.2$  Hz,  $J = 1.6$  Hz), 4.03 (m, 4H), 3.77 (dd, 1H,  $J = 7.0$  Hz,  $J = 1.6$  Hz), 3.31 (s, 1H), 1.42 (s, 3H), 1.39 (s, 3H), 1.37 (s, 3H), 1.30 (s, 3H).  $^{13}\text{C}$  NMR (125 MHz,  $\text{CDCl}_3$ )  $\delta$  (ppm): 170.8, 111.0, 109.3, 78.7, 76.2, 74.9, 70.0, 66.7, 26.7, 26.6, 26.1, 25.3. HRMS (LDI/TOF)  $m/z$   $[\text{M} + \text{H}]^+$  calc.: 291.1556 found: 291.0980.

### 2.2.3 | Synthesis of ligands 7 and 8

Ligands **7** and **8** were obtained by reacting the products **5** and **6**, respectively, with  $\text{CS}_2$  in basic medium, as described by Manjunatha (Manjunatha, Poojary, Lobo, Fernandes, & Kumari, 2010). In a 10 ml round-bottom flask, 80 mg of NaOH was dissolved in 3 ml of ethanol, and then, 300 mg of **5** or **6** was added along with 1 ml of  $\text{CS}_2$ . The reacting mixture was stirred at 45°C during 24 hr. The solvent and excess of  $\text{CS}_2$  were evaporated under reduced pressure. The

residue was extracted using dichloromethane and brine, by dropwise addition of aqueous 0.1 M HCl until pH = 5. The organic phase was dried over sodium sulfate and then filtered. Compounds **7** and **8** were purified by column chromatography and obtained in 58 and 78% yield, respectively.

Ligand 1,3,4-Oxadiazolidine-2-thione **7**: oil,  $\mu$ : 72.56 mPa s,  $\rho$ : 1.354 g/cm<sup>3</sup>, IR (KBr)  $\nu$ (cm<sup>-1</sup>): 3,500–3,300 (br, O–H stretch), 3,317 (m, NH stretch), 2,990 and 2,926 (m, CH<sub>aliphatic</sub> asymmetric/symmetric stretch), 1,652 (s, C=N stretch), 1,260, 1,210, 1,160, 1,140, 1,080 (m, s, ketal C–C stretch). <sup>1</sup>H NMR (500 MHz, CDCl<sub>3</sub>)  $\delta$ (ppm): 11.27 (s, 1H), 4.93 (s, 1H), 4.28 (dd, 1H,  $J$  = 7.9 Hz,  $J$  = 2.4 Hz), 4.17 (dd, 1H,  $J$  = 8.7 Hz,  $J$  = 6.0 Hz), 4.07 (ddd, 1H,  $J$  = 8.9 Hz,  $J$  = 6.0 Hz,  $J$  = 4.6 Hz), 3.98 (dd, 1H,  $J$  = 8.8 Hz,  $J$  = 4.6 Hz), 3.94 (dd, 1H,  $J$  = 8.8 Hz,  $J$  = 8.0 Hz), 3.49 (s, 1H), 1.42 (s, 3H), 1.39 (s, 3H), 1.38 (s, 3H), 1.33 (s, 3H). <sup>13</sup>C NMR (125 MHz, CDCl<sub>3</sub>)  $\delta$ (ppm): 178.7, 162.8, 111.1, 110.4, 80.1, 76.9, 76.8, 67.8, 65.4, 27.1, 26.7, 26.5, 25.1. HRMS (LDI/TOF)  $m/z$  [M + H]<sup>+</sup> calc.: 333.1120 found: 333.1031.

Ligand 1,3,4-Oxadiazolidine-2-thione **8**: oil,  $\mu$ : 60.11 mPa s,  $\rho$ : 1.276 g/cm<sup>3</sup>, IR (KBr)  $\nu$ (cm<sup>-1</sup>): 3,445 (br, O–H stretch), 3,161 (w, NH stretch), 2,985 and 2,934 (m, CH<sub>aliphatic</sub> asymmetric/symmetric stretch), 1,496 (s, C=N stretch), 1,260, 1,210, 1,160, 1,070 (s, m, ketal C–C stretch). <sup>1</sup>H NMR (500 MHz, CDCl<sub>3</sub>)  $\delta$  (ppm): 5.01 (d, 1H,  $J$  = 7.9 Hz), 4.63 (dd, 1H,  $J$  = 7.9 Hz,  $J$  = 3.6 Hz), 4.16 (m, 1H), 4.07 (m, 2H), 3.64 (dd, 1H,  $J$  = 7.1 Hz,  $J$  = 3.6 Hz), 1.53 (s, 3H), 1.52 (s, 3H), 1.42 (s, 3H), 1.33 (s, 3H). <sup>13</sup>C NMR (125 MHz, CDCl<sub>3</sub>)  $\delta$ (ppm) 178.7, 161.2, 112.3, 109.9, 78.8, 75.8, 70.9, 70.0, 66.9, 26.7, 26.6, 26.0, 25.1. HRMS (LDI/TOF)  $m/z$  [M + H]<sup>+</sup> calc.: 333.1120 found: 333.2360.

## 2.2.4 | Synthesis of gold complexes **9** to **12**

In a 10 ml round-bottom flask were added 0.1 mmol of starting material (either **7** or **8**) and then dissolved in 4 ml of dichloromethane along with 0.1 mmol of NaHCO<sub>3</sub>. After that, 0.1 mmol of [Au(PEt<sub>3</sub>)Cl] (to produce **9** and **10**) or [Au(PPh<sub>3</sub>)Cl] (to produce **11** and **12**) was added and the reaction mixture was left under inert atmosphere and magnetic stirring for 24 hr, at room temperature and protected from light. At the end of the reaction, the solvent was evaporated under reduced pressure and the product was purified by column chromatography, while protected from light. Compounds **9**, **10**, **11**, and **12** were obtained in 85%–90% yield and kept at –20°C protected from light.

Complex **9**: oil, BP: ND,  $\mu$ : 125.03 mPa s,  $\rho$ : 1.242 g/cm<sup>3</sup>, IR (KBr)  $\nu$ (cm<sup>-1</sup>): 3,300 (br, O–H stretch), 2,990 and 2,930 (m, CH<sub>aliphatic</sub> asymmetric/symmetric stretch), 1,450 (s, P–C deformation), 1,250, 1,210, 1,165, 1,085 (s, m, ketal C–C stretch). <sup>1</sup>H NMR (500 MHz, CDCl<sub>3</sub>)  $\delta$ (ppm): 4.99 (d, 1H,  $J$  = 2.4 Hz), 4.30 (dd, 1H,  $J$  = 7.3 Hz,  $J$  = 2.6 Hz),

4.16 (dd, 1H,  $J$  = 8.6 Hz,  $J$  = 5.7 Hz), 4.06 (ddd, 1H,  $J$  = 8.7 Hz,  $J$  = 5.6 Hz,  $J$  = 4.8 Hz), 4.02 (dd, 1H,  $J$  = 8.6 Hz,  $J$  = 7.4 Hz), 3.96 (dd, 1H,  $J$  = 8.6 Hz,  $J$  = 4.7 Hz), 1.90 (dq, 6H,  $J$  = 10.0 Hz,  $J$  = 7.6 Hz), 1.42 (s, 3H), 1.38 (s, 3H), 1.37 (s, 3H), 1.34 (s, 3H), 1.24 (dt, 9H,  $J$  = 18. Hz,  $J$  = 7.6 Hz). <sup>13</sup>C NMR (125 MHz, CDCl<sub>3</sub>)  $\delta$ (ppm): 171.1, 164.9, 110.4, 110.0, 80.8, 77.0, 76.9, 67.9, 65.5, 27.1, 26.7, 26.5, 25.2, 17.9 (d, 3C,  $J$  = 34.2 Hz), 9.0 (s, 3C). <sup>31</sup>P NMR (202 MHz, CDCl<sub>3</sub>)  $\delta$ (ppm): 36.67. HRMS (LDI/TOF)  $m/z$  [M + H]<sup>+</sup> calc.: 647.1618 found: 647.4000.

Complex **10**: oil, BP: ND,  $\mu$ : 104.95 mPa s,  $\rho$ : 1.240 g/cm<sup>3</sup>, IR (KBr)  $\nu$ (cm<sup>-1</sup>): 3,350 (br, O–H stretch), 2,985 and 2,935 (m, CH<sub>aliphatic</sub> asymmetric/symmetric stretch), 1,450 (s, P–C deformation), 1,255, 1,215, 1,140, 1,075 (s, m, ketal C–C stretch). <sup>1</sup>H NMR (500 MHz, CDCl<sub>3</sub>)  $\delta$ (ppm): 5.09 (d, 1H,  $J$  = 7.9 Hz), 4.68 (dd, 1H,  $J$  = 7.8 Hz,  $J$  = 2.8 Hz), 4.06 (m, 3H), 3.58 (td, 1H,  $J$  = 7.3 Hz,  $J$  = 2.3 Hz), 2.73 (d, 1H,  $J$  = 7.2 Hz), 1.89 (dq, 6H,  $J$  = 10.0 Hz,  $J$  = 7.6 Hz), 1.47 (s, 3H), 1.46 (s, 3H), 1.35 (s, 3H), 1.28 (s, 3H), 1.24 (dt, 9H,  $J$  = 18.8 Hz,  $J$  = 7.6 Hz). <sup>13</sup>C NMR (125 MHz, CDCl<sub>3</sub>)  $\delta$ (ppm): 170.9, 163.6, 111.4, 109.4, 78.7, 76.0, 70.3, 70.0, 66.9, 26.8, 26.7, 26.2, 25.2, 17.9 (d, 3C,  $J$  = 34.3 Hz), 9.0 (s, 3C). <sup>31</sup>P NMR (202 MHz, CDCl<sub>3</sub>)  $\delta$ (ppm): 36.63. HRMS (LDI/TOF)  $m/z$  [M + H]<sup>+</sup> calc.: 647.1618 found: 647.3910.

Complex **11**: oil, BP: ND,  $\mu$ : 88.53 mPa s,  $\rho$ : 1.389 g/cm<sup>3</sup>, IR (KBr)  $\nu$ (cm<sup>-1</sup>): 3,400 (br, O–H stretch), 3,060 (w, C–H<sub>aromatic</sub> stretch), 2,990, 2,940 (m, CH<sub>aliphatic</sub> asymmetric/symmetric stretch), 1,460 (m, aromatic C–C stretch), 1,450 (m, P–C deformation), 1,265, 1,215, 1,080 (s, m, ketal C–C stretch), 750 (s, aromatic out-of-plane C–H bending), 537 (s, aromatic P–C stretch). <sup>1</sup>H NMR (500 MHz, CDCl<sub>3</sub>)  $\delta$ (ppm): 7.55 (m, 15H), 5.03 (d, 1H,  $J$  = 2.6 Hz), 4.34 (dd, 1H,  $J$  = 7.3 Hz,  $J$  = 2.6 Hz), 4.17 (dd, 1H,  $J$  = 8.6 Hz,  $J$  = 5.7 Hz), 4.07 (ddd, 1H,  $J$  = 8.7 Hz,  $J$  = 5.7 Hz,  $J$  = 4.8 Hz), 4.03 (dd, 1H,  $J$  = 8.7 Hz,  $J$  = 7.4 Hz), 3.97 (dd, 1H,  $J$  = 8.6 Hz,  $J$  = 4.7 Hz), 1.42 (s, 3H), 1.38 (s, 3H), 1.37 (s, 3H), 1.34 (s, 3H). <sup>13</sup>C NMR (126 MHz, CDCl<sub>3</sub>)  $\delta$ (ppm): 171.5, 164.8, 134.2 (d, 6C,  $J$  = 13.8), 131.9 (d, 3C,  $J$  = 2.4), 129.3 (d, 6C,  $J$  = 11.7), 128.8 (d, 3C,  $J$  = 58.9), 110.4, 110.1, 80.8, 77.1, 76.9, 67.9, 65.5, 27.1, 26.7, 26.5, 25.2. <sup>31</sup>P NMR (202 MHz, CDCl<sub>3</sub>)  $\delta$ (ppm): 37.63. HRMS (LDI/TOF)  $m/z$  [M + H]<sup>+</sup> calc.: 791.1618 found: 791.5861.

Complex **12**: oil, BP: ND,  $\mu$ : 95.68 mPa s,  $\rho$ : 1.261 g/cm<sup>3</sup>, IR (KBr)  $\nu$ (cm<sup>-1</sup>): 3,300 (br, O–H stretch), 3,060 (w, aromatic C–H stretch), 2,985, 2,935 (m, s CH<sub>aliphatic</sub> asymmetric/symmetric stretch), 1,440 (s, aromatic C–C stretch), 1,265, 1,215, 1,075 (m, ketal C–C stretch), 735 (s, aromatic out-of-plane C–H bending), 540 (s, aromatic P–C stretch). <sup>1</sup>H NMR (500 MHz, CDCl<sub>3</sub>)  $\delta$ (ppm): 7.54 (m, 15H), 5.15 (d, 1H,  $J$  = 7.8 Hz), 4.74 (dd, 1H,  $J$  = 7.8 Hz,  $J$  = 2.8 Hz), 4.05 (m); 3.63 (d, 1H,  $J$  = 4.8 Hz), 2.48 (s, 1H), 1.50 (s, 3H), 1.45 (s, 3H), 1.36 (s, 3H), 1.30 (s, 3H). <sup>13</sup>C NMR (126 MHz, CDCl<sub>3</sub>)  $\delta$ (ppm): 170.6, 163.7, 134.2 (d, 6C,  $J$  = 13.7 Hz), 131.9 (d,

3C,  $J = 2.5$  Hz), 129.3 (d, 6C,  $J = 11.6$  Hz), 128.8 (d, 3C,  $J = 58.9$  Hz), 111.5, 109.5, 78.7, 76.0, 70.5, 70.1, 66.9, 26.8, 26.7, 26.2, 25.3.  $^{31}\text{P}$  NMR (202 MHz,  $\text{CDCl}_3$ )  $\delta$ (ppm): 37.65. HRMS (LDI/TOF)  $m/z$   $[\text{M} + \text{H}]^+$  calc.: 791.1618 found: 791.5796.

## 2.3 | Biological activity assays

### 2.3.1 | Cytotoxicity assay against tumor and non-tumor cell lines

Cytotoxic activity was tested against the following tumor cell lines: 4T1 (murine mammary carcinoma) and B16-F10 (mouse metastatic skin melanoma). Baby hamster kidney BHK-21 was used as non-tumoral cell line. Drug activity was measured by assessing the inhibitory concentration that led to apoptosis of 50% of growing cells ( $\text{IC}_{50}$ ). Cell lines were axenically propagated in complete RPMI 1640 culture medium at pH 7.4, supplemented with 10% of heat-inactivated fetal bovine serum (FBS), 4 mM HEPES, 14 mM  $\text{NaHCO}_3$ , 0.27 mM ampicillin, and 0.06 mM streptomycin in 5% (v/v)  $\text{CO}_2$  humid atmosphere. Cells were rinsed with PBS/EDTA pH 7.4 buffer and harvested with trypsin 0.02% (v/v). Trypsin was then inactivated by adding 1.5 ml of complete RPMI where cells were seeded in 96-well tissue culture plates at the following densities:  $0.5 \times 10^3$  (BHK-21),  $1.5 \times 10^3$  (B16-F10) and  $2.0 \times 10^3$  (4T1) cells/well/100  $\mu\text{l}$  and incubated at 37°C in a humidified atmosphere containing 5%  $\text{CO}_2$  during 24 hr for complete adherence.

DMSO solutions of the tested compounds were serially diluted (from 100 to 0.1  $\mu\text{M}$ ) in RPMI cell culture medium (< 1% DMSO) in quadruplicate. The negative control was obtained with cells exposure in RPMI 1640 medium supplemented with 10% FBS. After 72 hr drug exposure, cells were incubated with 3-(4,5-dimethyl-2-thiazolyl)-2,5-diphenyl-2H-tetrazolium bromide, MTT (Sigma-Aldrich #M2128) (5  $\mu\text{g}/10 \mu\text{l}$ /well) for 4 hr at 37°C in 5%  $\text{CO}_2$  humid atmosphere. The supernatant was then removed by aspiration, and 100  $\mu\text{L}$  of DMSO/well was added. Cell viability was determined by absorbance at 570 nm (using a plate spectrophotometer) of the obtained solution which contains formazan salts, a product of mitochondrial reduction of MTT by viable cells (Mosmann, 1983).

### 2.3.2 | Antileishmanial assays against intracellular amastigotes

*Leishmania (Viannia) braziliensis* (strain MHOM/BR/1994/H3227) promastigotes were maintained in minimum essential culture medium ( $\alpha$ -MEM) (Gibco, Invitrogen NY, USA) supplemented with 10% (v/v) heat-inactivated FBS (Cultilab,

Campinas, SP, Brazil), 100 mg/ml kanamycin, 50 mg/ml ampicillin, 2 mM L-glutamine, 5 mg/ml hemin, and 5 mM biotin (Sigma-Aldrich #B2517), at pH 7.0 and incubated at 25°C. *L. braziliensis* (MHOM/BR/94/H3227) and *L. infantum* (MHOM/MA/67/ITMAP-263) parasites expressing firefly luciferase as a reporter gene (pSP72 $\alpha$ HYG $\alpha$ LUC1.2)—*LbrLUC* and *LinLUC*. Transfections were performed as previously described (Roy et al., 2000). Human monocyte-derived macrophage cell line THP-1 was maintained in RPMI 1640 medium supplemented with 10% FBS. Cells were plated in blank 96-well tissue culture plate at  $8 \times 10^5$  cells/mL and differentiated by incubating with 20 ng/ml of phorbol 12-myristate 13-acetate—PMA (Sigma-Aldrich, #P8139) at 37°C in a 5%  $\text{CO}_2$  containing humid atmosphere for 3 days. Cells were washed with RPMI medium and subsequently infected with *LbrLUC* or *LinLUC* at a parasite/macrophage ratio of 10:1 for 3 hr. Non-internalized parasites were removed by three washes with HEPES/NaCl buffer (20 mM HEPES, 0.15 M NaCl, 10 mM glucose, pH 7.2). After 3 days, RPMI was aspirated and the luciferase activity assessed by adding 20  $\mu\text{l}$  of reconstituted ONE-Glo™ Luciferase Assay System solution as enzyme substrate, following manufacturer's instructions (Promega; #E6110). Luciferase activity was measured by luminescence detection in a luminometer SpectraMax M5 (Molecular Devices) using 1-s integration/well. Non-infected THP-1 macrophages were considered as signal background while non-treated infected THP-1 cells were used as a control for growth comparison. Amphotericin B and miltefosine were added as a positive control.

### 2.3.3 | Cytotoxicity assay against human macrophage cell line

In vitro cytotoxicity activity was evaluated by quantifying the ability of living cells to reduce the yellow dye MTT (Sigma-Aldrich #M2128) to a purple formazan product (Mosmann, 1983). Cytotoxicity (cell viability) was evaluated on human monocyte-derived THP-1 macrophage cell lines. For macrophage differentiation,  $5 \times 10^5$  precursor monocytes/well were seeded in 96-well plates treated with 20 ng/ml phorbol 12-myristate 13-acetate PMA (Sigma-Aldrich #P8139) and incubated 48 hr at 37°C in 5%  $\text{CO}_2$  humid atmosphere. Stock solutions of gold(I) complexes were prepared in DMSO and serially diluted in RPMI medium (<1% DMSO). After 72 hr of drug exposure at 37°C and 5%  $\text{CO}_2$ , cells were incubated with MTT (10 mM in water solution—10  $\mu\text{l}$ /well) for 4 hr at 37°C and 5%  $\text{CO}_2$ . MTT is metabolized by viable cells resulting in a purple product that after being solubilized in 100  $\mu\text{l}$  of DMSO can be quantified through colorimetric assay using a plate reader (absorbance at 570 nm). Negative control was performed considering untreated cells in RPMI 1640.

Compound	Tumor cells IC <sub>50</sub> (μM ± SD)				Non-tumor cell IC <sub>50</sub> (μM ± SD)
	B16-F10	SI <sup>a</sup>	4T1	SI <sup>a</sup>	BHK-21
7	>100	ND	>100	ND	>100
8	>100	ND	>100	ND	>100
9	2.0 ± 0.2	10.6	3.9 ± 0.3	5.4	21.2 ± 0.3
10	3.2 ± 0.2	6.9	2.6 ± 0.2	8.5	22.2 ± 0.9
11	8.3 ± 0.1	2.7	3.6 ± 0.3	6.2	22.3 ± 0.4
12	7.1 ± 0.5	3.3	3.9 ± 0.1	6.1	23.6 ± 0.8
Cisplatin	6.4 ± 1.0	2.8	6.2 ± 2.3	2.9	18.1 ± 3.0
AuPPh <sub>3</sub> Cl	6.6 ± 0.1	3.4	10.3 ± 2.3	2.4	23.0 ± 0.3
AuPEt <sub>3</sub> Cl	2.3 ± 0.5	9.7	9.5 ± 1.1	2.4	22.5 ± 0.2

Note: IC<sub>50</sub> are presented in μM and SD-standard deviation of three independent experiments.

Abbreviations: ND, not determined; SD, standard deviation.

<sup>a</sup>SI: selectivity index estimated by the ratio: IC<sub>50,tumor</sub>/IC<sub>50 non-tumor</sub>

**TABLE 1** Anticancer activity profile of gold(I) complexes expressed as 50% inhibitory concentration (IC<sub>50</sub>) of compounds **7–12** against 4T1 (murine mammary carcinoma), B16-F10 (mouse metastatic skin melanoma), along with their selectivity index (SI) compared to non-tumor cell BHK-21 (baby hamster kidney)

### 2.3.4 | Statistical analyses

IC<sub>50</sub> and CC<sub>50</sub> values were calculated based on concentration–response curves applying a sigmoidal concentration–response equation with variable slope carried out using the software GraphPad Prism version 6.0 (GraphPadSoftware Inc.). Selectivity index was estimated by the ratio CC<sub>50</sub>/IC<sub>50</sub>. When applied, data were analyzed by analysis of variance (ANOVA) followed by Tukey's multicomparison test. A *p* value <.05 was considered statistically significant.

## 3 | RESULTS AND DISCUSSION

### 3.1 | Synthesis of gold(I) complexes

In the <sup>1</sup>H NMR spectra of ligand **7**, we observe the presence of the signal corresponding to the heterocyclic NH hydrogen at 11.27 ppm, although this signal is not readily observable in the <sup>1</sup>H NMR spectra of **8**, due to its characteristic broadness. Also, the signals previously present in the <sup>1</sup>H NMR spectra of the starting materials **5** and **6**, at 8.84 and 4.27 ppm, and at 8.03 and 3.31 ppm, respectively, corresponding to the hydrazide group hydrogens, are no longer present, thus suggesting the formation of the desired compounds **7** and **8**. Also, we observe in the <sup>13</sup>C NMR spectra of **7** and **8** that, instead of signals at 170.0 and 170.8 ppm (corresponding to the carbonyl carbons), respectively, we observe new signals at 178.7 and 162.8 ppm for **7** and at 178.7 and 161.2 ppm for **8**, corresponding to the C=N and the C=S carbons, respectively. Also important, the IR spectra of **5** and **6** differ of **7** and **8** in many points such as some variation in the absorption

bands corresponding to NH<sub>2</sub> stretch, replaced instead by the single NH stretching band around 3,300 cm<sup>-1</sup>. These observations, along with mass spectrometry, provide evidence for the formation of **7** and **8**.

In the <sup>1</sup>H NMR spectra of **9** and **10**, we observe at 1.90 and 1.24 ppm (for **9**) and at 1.89 and 1.24 ppm (for **10**) the signals for the methylene and methyl hydrogens, respectively, corresponding to the phosphine moiety of the molecule. We can also observe in the <sup>13</sup>C NMR spectra of **9** and **10** the signals of the methylene and methyl carbons adjacent to the phosphorous atom, namely at 17.97 and 9.09 ppm for **9** and at 17.93 and 9.09 ppm for **10**. Furthermore, the IR spectra of **9** and **10** both show the characteristic deformation band of the P–C bond, at 1,450 cm<sup>-1</sup>. These results are expected for the synthesized compounds. Finally, if we pay close attention to the <sup>1</sup>H NMR spectra of **9** and **10** and compare it to that of its precursors **7** and **8**, we can readily observe that after coordination with gold(I), the relative positions of hydrogens 6' and 4 have been interchanged, that is, hydrogen 6' was originally located further down than hydrogen 4 in the <sup>1</sup>H NMR spectra of the ligands, whereas the opposite is true for the complexes.

In the <sup>1</sup>H NMR spectra of **11** and **12**, we observe the multiplets corresponding to the aromatic hydrogens at 7.55 and 7.54 ppm, respectively. We can also observe in the <sup>13</sup>C NMR spectra of **11** and **12** the signals of the aromatic carbons between 134.2 and 128.8 ppm in both cases. Also, the IR spectra of **11** and **12** both show the characteristic stretch band of the C–C aromatic bond, at 1,450 cm<sup>-1</sup>, as well as the characteristic out-of-plane bending of aromatic C–H at 750 cm<sup>-1</sup>. In a similar manner as with complexes **9** and **10**, we observe that after coordination with gold(I), the relative positions of hydrogens 6' and 4 between the <sup>1</sup>H NMR spectra of the ligands and the complexes are interchanged.

### 3.2 | Gold(I) complexes presented selective anticancer activity

All compounds showed higher selectivity indexes when compared to cisplatin (Table 1). None of the ligands (compounds **7** and **8**) showed cytotoxicity below 100  $\mu\text{M}$ . In the case of skin melanoma-derived cell line B16-F10, results show that complexes **9** and **10** (triethylphosphine derivatives) are more cytotoxic and selective than the triphenylphosphine analogue compounds **11** and **12**, presenting  $\text{IC}_{50}$  values of  $2.0 \pm 0.2$  and  $3.2 \pm 0.2$   $\mu\text{M}$ , with selectivity indexes of 10.6 and 6.9, respectively. Similar evidence was previously found in the literature, where triethylphosphine derivatives have shown better activity, possibly because of steric factors, a result that is consistent with past works of other leading authors (Chaves et al., 2014, 2015, 2016; de Almeida et al., 2017; Garcia et al., 2016). Furthermore, in the case of skin melanoma (B16-F10), if we compare the results for compounds **9** and **10**, we see that compound **9** is slightly more active than compound **10** (with  $\text{IC}_{50}$  of  $2 \pm 0.2$ ,  $\mu\text{M}$  compared to  $3.2 \pm 0.2$   $\mu\text{M}$  from compound **10**). On the other hand, results obtained from the mammary carcinoma (4T1) tests are quite scattered and do not show any immediate pattern that could allow us to establish a satisfying structure–activity relation. It is very important to notice that the ligands showed cytotoxicity only after coordination with gold(I) and also that the starting gold material alone already presented some activity, yet it became more selective and more active after complexation with some of the gluco-derived moieties.

### 3.3 | Gold(I) complexes are antileishmanial agents less toxic than their metal precursors

Gold(I) complexes **9**, **10**, **11**, and **12** were able to impair the proliferation of *L. braziliensis* intramacrophagic amastigotes in vitro with mean  $\text{IC}_{50}$  values of 3  $\mu\text{M}$ , the same range as those shown by their gold(I) precursors  $\text{AuPET}_3\text{Cl}$ —gold(I) triethylphosphine chloride—and  $\text{AuPPh}_3\text{Cl}$ —gold(I) triphenylphosphine chloride (Table 2 and Figure 2). Considering their cytotoxicity against THP-1 host macrophages, the gold(I) complexes were 4 to 6 times more selective toward the parasite than their metal precursor counterparts alone, which showed SI values around 2 (Table 2). This is consistent with the fact that all four gold(I) complexes were around 3 times less toxic to the host macrophage than the free  $\text{AuPET}_3\text{Cl}$  and  $\text{AuPPh}_3\text{Cl}$  (Table 2 and Figure 2). Complexes **10** and **12**, derived from methyl (2,3)/(5,6)-di-*O*-isopropylidene-D-gluconate **4**—were both less toxic to the host macrophages when compared to complexes **9** and **11**, synthesized from the ligand isomer methyl (3,4)/(5,6)-di-*O*-isopropylidene-D-gluconate **3** (Table 2). This hexose-driven differential cytotoxicity is quite intriguing, since THP-1 human macrophages do

**TABLE 2** Antileishmanial activity and selectivity index of gold(I) complexes based on oxadiazolidine-2-thione and D-gluconate ligands against *Leishmania braziliensis* intracellular amastigotes and THP-1 human macrophage cell line

Compound	$\text{IC}_{50}$ $\mu\text{M}$ (95% CI)	$\text{CC}_{50}$ $\mu\text{M}$ (95% CI)	SI
	<i>L. braziliensis</i> intracellular amastigotes	THP-1 macrophages	
7	>10	ND	ND
8	>10	ND	ND
9	3.09 (2.78–3.42)	15.1 (13.7–16.66)	4.9
10	3.3 (2.98–3.65)	19.44 (17.52–21.57)	5.9
11	2.96 (2.39–3.67)	11.77 (10.87–12.75)	4
12	3.27 (2.34–4.57)	19.3 (17.58–21.17)	6
$\text{AuPPh}_3\text{Cl}$	2.83 (2.57–3.12)	4.98 (4.64–5.33)	1.7
$\text{AuPET}_3\text{Cl}$	3.31 (2.79–3.93)	5.43 (5.08–5.79)	1.6
Miltefosine	6.68 (5.55–8.03)	39.08 (37.65–40.57)	5.85
AmB	0.12 (0.10–0.15)	12 (11.43–12.59)	100

Note:  $\text{IC}_{50}$  and  $\text{CC}_{50}$  are presented in  $\mu\text{M}$  and 95% CI—confidence interval.

Abbreviations: 95% CI, 95% confidence interval; AmB, amphotericin B; ND, not determined; SI: selectivity index estimated by the ratio  $\text{CC}_{50}/\text{IC}_{50}$ .

express different forms of glucose transporters (Fu, Maianu, Melbert, & Garvey, 2004). Additionally, as intracellular parasites, it is expected that a good antileishmanial agent should be able to pass through the macrophage's membrane to become available against *Leishmania* inside the cell. It is no surprise that the most widely used drugs against leishmaniasis are antimony-derived sugar-based molecules: sodium stibogluconate and meglumine antimoniate (El Fadili et al., 2008; Frézard, Demicheli, & Ribeiro, 2009). Inspired by these facts, efforts have been made to employ this “Trojan horse” strategy in antileishmanial metallodrug-based chemotherapy (Ferreira et al., 2010, 2014). Thus, these four less toxic D-gluconate-derived gold(I) complexes represent potential antileishmanial agents that deserve attention in further drug development studies, including sugar-mediated drug delivery strategies. Although no difference in terms of antileishmanial activity was observed between the gold(I) complexes and their precursors, the former's synthesis is justified by their lesser toxicity against THP-1 human macrophages, which directly impact drug selectivity.

Unlike the anticancer profile presented in this study—where triethylphosphine-substituted gold(I) complexes **9** and **10** were more active against metastatic skin melanoma-derived cell line B16-F10 than triphenylphosphine-based complexes **11** and **12** (Table 1)—the structure of the phosphine group used, either triphenylphosphine ( $\text{PPh}_3$ ) or triethylphosphine ( $\text{PET}_3$ ), had no impact on the

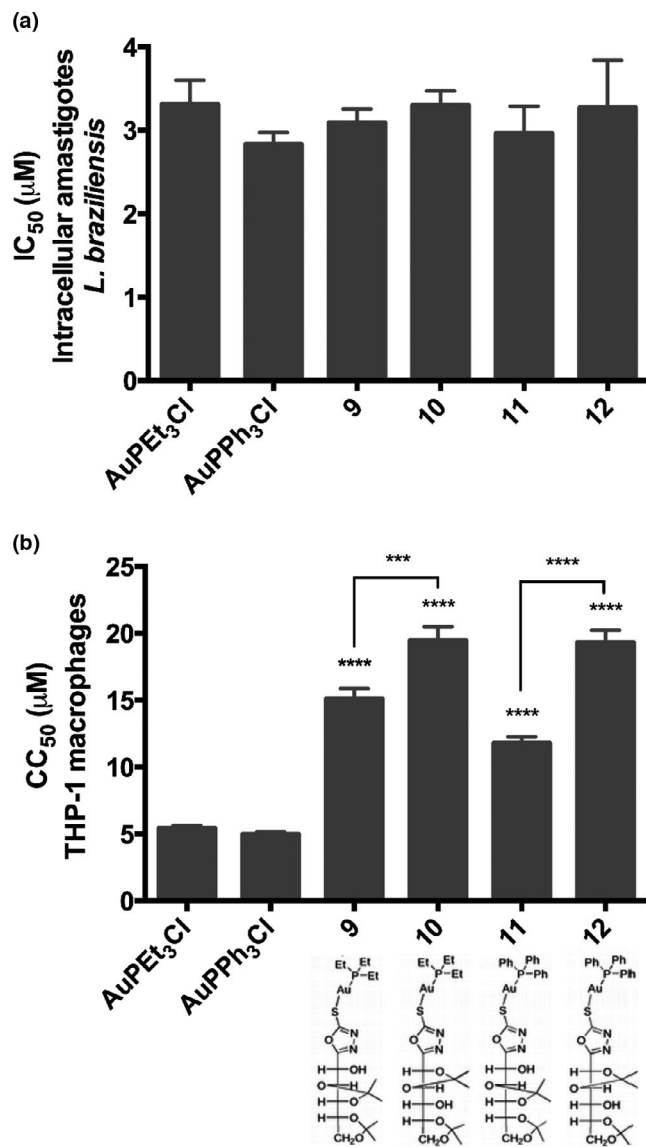


**FIGURE 2** Antileishmanial and cytotoxic activity of gold(I) complexes with oxadiazolidine-2-thione and D-gluconate ligands. (a) The IC<sub>50</sub> against *Leishmania braziliensis* intracellular amastigotes was calculated based on concentration–response curves and shown here to compare antileishmanial activity among the gold(I) complexes and their precursors AuPEt<sub>3</sub>Cl and AuPPh<sub>3</sub>Cl. (b) The cytotoxic concentration that kills 50% of THP-1 human macrophages (CC<sub>50</sub>) was compared, highlighting that the four gold(I) complexes were 3x less toxic than their free metal precursor. Complexes **10** and **12**—derived from methyl (3,4)/(5,6)-di-*O*-isopropylidene-D-gluconate **3**—were either less toxic when compared to complexes **9** and **11**, synthesized from the ligand isomer methyl (2,3)/(5,6)-di-*O*-isopropylidene-D-gluconate **4**. AuPEt<sub>3</sub>Cl: gold(I) triethylphosphine chloride; AuPPh<sub>3</sub>Cl: gold(I) triphenylphosphine chloride. Statistical differences were calculated using ANOVA one-way followed by Tukey's multiple comparison test. \*\*\**p* = .001; \*\*\*\**p* = .0001

structure–activity relationship when tested against intramacrophagic *L. braziliensis* amastigotes (Table 2 and Figure 2). This was also a surprise for the rest of our

research team, since we had been observing this PPh<sub>3</sub>/PET<sub>3</sub>-dependent biological response in gold(I) complexes with different ligands (Chaves et al., 2015; Garcia et al., 2016). Instead, we found that a slight isomeric variation in the D-gluconate ligand was enough to drive a higher cytotoxic effect. This also highlights the importance of using different cell types to infer about biological activities in drug discovery and drug development studies.

The complexes' antileishmanial activity at low micromolar range against *L. braziliensis* raises the question on how would they behave against other *Leishmania* species, and also opens the possibility for them be considered as a potential solution against both cutaneous and visceral leishmaniasis. In fact, we recently observed that gold(I) complexes show very similar antileishmanial activity among different *Leishmania* species (Chaves et al., 2016). Gold(I)-containing heterocyclic complexes were also active against *L. infantum*, the main etiological agent of visceral leishmaniasis (Zhang et al., 2018). A previous study demonstrates that gold(I)-based compound auranofin presented antileishmanial activity both in vitro and in vivo against cutaneous leishmaniasis-causing species *L. amazonensis* and *L. major* (Sharlow et al., 2014). In this context, we had expected that gold(I) derivatives were actually active in a wide spectrum against different *Leishmania* spp.

## 4 | CONCLUSIONS

In this work, two ligands and four gold(I) complexes were synthesized, characterized, and evaluated for anticancer and antileishmanial properties. All tested gold(I) complexes are potential anticancer and antileishmanial drug candidates that should be further investigated. For both biological activities explored in this work, the complexation of the ligands with gold(I) somehow improved drug activity (or reduced toxicity against control cell), since neither ligand was biologically active by itself. We thus reinforce the fact that mechanistic approach studies are encouraged in order to further support drug development follow-up. Such studies could help to demonstrate the potential application of oxadiazolidine-based gold(I) complexes as anticancer and antileishmanial drugs. Since we observed an anticancer property dependent on the triethylphosphine substitution, the evaluation of compounds with different phosphine ligands should help us establish a more consistent structure–activity relation, aimed toward higher efficacy and selectivity. Additionally, these novel gold(I) complexes could be considered for combined chemotherapy in anticancer and antileishmanial treatment, because both the 1,3,4-oxadiazole and gold(I) itself can act as anti-inflammatory agents and help immune response to tackle both tumor cells and *Leishmania* parasites.

## ACKNOWLEDGMENTS

Thanks to Dr. Silvia Uliana, University of São Paulo, Brazil, who kindly provided the *L. braziliensis* H3227 expressing luciferase as reporter. The authors wish to thank Fapemig, CNPq, and UFJF for financial support. This work was financed in part by the Coordenação de Aperfeiçoamento de Pessoal de Nível Superior—Brazil (CAPES)—Finance Code 88881.133591/2016-01. This study was also funded by Fapemig—APQ-03059-16. The authors also thank the Organization of American States for providing the scholarship that made this work possible.

## CONFLICT OF INTEREST

There are no conflicts of interest of any of the parts involved in this work.

## DATA AVAILABILITY STATEMENT

I confirm that my article contains a Data Availability Statement. Detailed transcripts are included in the article so that analyses can be validated. For additional data, contact the correspondence author.

## ORCID

Rubens L. do Monte-Neto  <https://orcid.org/0000-0002-4688-2462>

Heveline Silva  <https://orcid.org/0000-0003-3537-4961>

## REFERENCES

- Baenziger, N. C., Bennett, W. E., & Soborofe, D. M. (1976). Chloro(triphenylphosphine)gold(I). *Acta Crystallographica Section B*, 32(3), 962–963. <https://doi.org/10.1107/S0567740876004330>
- Chaves, J. D. S., Damasceno, J. L., Paula, M. C. F., de Oliveira, P. F., Azevedo, G. C., Matos, R. C., ... de Almeida, M. V. (2015). Synthesis, characterization, cytotoxic and antitubercular activities of new gold(I) and gold(III) complexes containing ligands derived from carbohydrates. *BioMetals*, 28(5), 845–860. <https://doi.org/10.1007/s10534-015-9870-8>
- Chaves, J. D. S., Neumann, F., Francisco, T. M., Corrêa, C. C., Lopes, M. T. P., Silva, H., ... de Almeida, M. V. (2014). Synthesis and cytotoxic activity of gold(I) complexes containing phosphines and 3-benzyl-1,3-thiazolidine-2-thione or 5-phenyl-1,3,4-oxadiazole-2-thione as ligands. *Inorganica Chimica Acta*, 414, 85–90. <https://doi.org/10.1016/j.ica.2014.01.042>
- Chaves, O. A., Jesus, C. S. H., Cruz, P. F., Sant'Anna, C. M. R., Brito, R. M. M., & Serpa, C. (2016). Evaluation by fluorescence, STD-NMR, docking and semi-empirical calculations of the o-NBA photo-acid interaction with BSA. *Spectrochimica Acta Part A: Molecular and Biomolecular Spectroscopy*, 169, 175–181. <https://doi.org/10.1016/j.saa.2016.06.028>
- da Silva Maia, P. I., Deflon, V. M., & Abram, U. (2014). Gold(III) complexes in medicinal chemistry. *Future Medicinal Chemistry*, 6(13), 1515–1536. <https://doi.org/10.4155/fmc.14.87>
- de Almeida, A. M., de Oliveira, B. A., de Castro, P. P., de Mendonça, C. C., Furtado, R. A., Nicolella, H. D., ... de Almeida, M. V. (2017). Lipophilic gold(I) complexes with 1,3,4-oxadiazol-2-thione or 1,3-thiazolidine-2-thione moieties: Synthesis and their cytotoxic and antimicrobial activities. *BioMetals*, 30(6), 841–857. <https://doi.org/10.1007/s10534-017-0046-6>
- El Fadili, K., Imbeault, Michaël, Messier, N., Roy, Gaétan, Gourbal, B., Bergeron, M., ... Ouellette, M. (2008). Modulation of gene expression in human macrophages treated with the anti-*Leishmania* pentavalent antimonial drug sodium stibogluconate. *Antimicrobial Agents and Chemotherapy*, 52(2), 526. <https://doi.org/10.1128/AAC.01183-07>
- Falcão, S. A. C., Jaramillo, T. M. G., Ferreira, L. G., Bernardes, D. M., Santana, J. M., & Favali, C. B. F. (2016). *Leishmania infantum* and *Leishmania braziliensis*: Differences and similarities to evade the innate immune system. *Frontiers in Immunology*, 7(287). <https://doi.org/10.3389/fimmu.2016.00287>
- Ferreira, C. S., Rocha, I. C. M. D., M. Neto, R. L., Melo, M. N., Frézard, F., & Demicheli, C. (2010). Influence of the nucleobase on the physicochemical characteristics and biological activities of SbV-ribonucleoside complexes. *Journal of the Brazilian Chemical Society*, 21, 1258–1265. <https://doi.org/10.1590/S0103-50532010000700013>
- Ferreira, W. A., Islam, A., Andrade, A. P. S., Fernandes, F. R., Frézard, F., & Demicheli, C. (2014). Mixed Antimony(V) complexes with different sugars to modulate the oral bioavailability of pentavalent antimonial drugs. *Molecules*, 19(5), 5478–5489. <https://doi.org/10.3390/molecules19055478>
- Frézard, F., Demicheli, C., & Ribeiro, R. R. (2009). Pentavalent antimonials: New perspectives for old drugs. *Molecules*, 14(7), 2317–2336. <https://doi.org/10.3390/molecules14072317>
- Fu, Y., Maianu, L., Melbert, B. R., & Garvey, W. T. (2004). Facilitative glucose transporter gene expression in human lymphocytes, monocytes, and macrophages: A role for GLUT isoforms 1, 3, and 5 in the immune response and foam cell formation. *Blood Cells, Molecules, and Diseases*, 32(1), 182–190. <https://doi.org/10.1016/j.bcmd.2003.09.002>
- Garcia, A., Machado, R. C., Grazul, R. M., Lopes, M. T. P., Corrêa, C. C., Dos Santos, H. F., ... Silva, H. (2016). Novel antitumor adamantane-azole gold(I) complexes as potential inhibitors of thioredoxin reductase. *JBIC Journal of Biological Inorganic Chemistry*, 21(2), 275–292. <https://doi.org/10.1007/s00775-016-1338-y>
- Leite de Oliveira, R., Deschoemaeker, S., Henze, A.-T., Debackere, K., Finisguerra, V., Takeda, Y., ... Mazzone, M. (2012). Gene-targeting of Phd2 improves tumor response to chemotherapy and prevents side-toxicity. *Cancer Cell*, 22(2), 263–277. <https://doi.org/10.1016/j.ccr.2012.06.028>
- Manjunatha, K., Poojary, B., Lobo, P. L., Fernandes, J., & Kumari, N. S. (2010). Synthesis and biological evaluation of some 1,3,4-oxadiazole derivatives. *European Journal of Medicinal Chemistry*, 45(11), 5225–5233. <https://doi.org/10.1016/j.ejmech.2010.08.039>
- Mosmann, T. (1983). Rapid colorimetric assay for cellular growth and survival: Application to proliferation and cytotoxicity assays. *Journal of Immunological Methods*, 65(1), 55–63. [https://doi.org/10.1016/0022-1759\(83\)90303-4](https://doi.org/10.1016/0022-1759(83)90303-4)
- Oliveira, G. (2014). Cancer and parasitic infections: Similarities and opportunities for the development of new control tools. *Revista Da Sociedade Brasileira De Medicina Tropical*, 47, 1–2. <https://doi.org/10.1590/0037-8682-0013-2014>
- Ott, I., Qian, X., Xu, Y., Vlecken, D. H. W., Marques, I. J., Kubutat, D., ... Bagowski, C. P. (2009). A Gold(I) phosphine complex containing a naphthalimide ligand functions as a TrxR inhibiting anti-proliferative agent and angiogenesis inhibitor. *Journal of Medicinal Chemistry*, 52(3), 763–770. <https://doi.org/10.1021/jm8012135>



- Patel, A. P., Tirosh, I., Trombetta, J. J., Shalek, A. K., Gillespie, S. M., Wakimoto, H., ... Bernstein, B. E. (2014). Single-cell RNA-seq highlights intratumoral heterogeneity in primary glioblastoma. *Science*, *344*(6190), 1396. <https://doi.org/10.1126/science.1254257>
- Regeling, H., de Rouville, E., & Chittenden, G. J. F. (1987). The chemistry of D-gluconic acid derivatives. Part 1: Synthesis of 3,4;5,6-di-O-isopropylidene-D-glucitol and 2,3;4,5-di-O-isopropylidene-aldehyde-D-arabinose from D-glucono-1,5-lactone. *Recueil des Travaux. Chimiques Des Pays-Bas*, *106*(8), 461–464. <https://doi.org/10.1002/recl.19871060805>
- Rigobello, M. P., Folda, A., Dani, B., Menabò, R., Scutari, G., & Bindoli, A. (2008). Gold(I) complexes determine apoptosis with limited oxidative stress in Jurkat T cells. *European Journal of Pharmacology*, *582*(1), 26–34. <https://doi.org/10.1016/j.ejphar.2007.12.026>
- Roy, G., Dumas, C., Sereno, D., Wu, Y., Singh, A. K., Tremblay, M. J., ... Papadopoulou, B. (2000). Episomal and stable expression of the luciferase reporter gene for quantifying *Leishmania* spp. infections in macrophages and in animal models. *Molecular and Biochemical Parasitology*, *110*(2), 195–206. [https://doi.org/10.1016/s0166-6851\(00\)00270-x](https://doi.org/10.1016/s0166-6851(00)00270-x)
- Sharlow, E. R., Leimgruber, S., Murray, S., Lira, A., Sciotti, R. J., Hickman, M., ... Lazo, J. S. (2014). Auranofin is an apoptosis-simulating agent with in vitro and in vivo anti-leishmanial activity. *ACS Chemical Biology*, *9*(3), 663–672. <https://doi.org/10.1021/cb400800q>
- Sundar, S., Jha, T. K., Thakur, C. P., Engel, J., Sindermann, H., Fischer, C., ... Berman, J. (2002). Oral miltefosine for Indian visceral Leishmaniasis. *New England Journal of Medicine*, *347*(22), 1739–1746. <https://doi.org/10.1056/NEJMoa021556>
- Tunes, L., Morato, R., Garcia, A., Schmitz, V., Steindel, M., Corrêa-Junior, J. D., ... Monte-Neto, R. L. (2020). Preclinical gold complexes as oral drug candidates to treat leishmaniasis are potent trypanothione reductase inhibitors. *ACS Infectious Diseases*, *6*, 1121–1139. <https://doi.org/10.1021/acscinfecdis.9b00505>
- Yeo, C. I., Ooi, K. K., Akim, A. M., Ang, K. P., Fairuz, Z. A., Halim, S. N. B. A., ... Tiekink, E. R. T. (2013). The influence of R substituents in triphenylphosphinegold(I) carbonimidothioates, Ph<sub>3</sub>PAu[SC(OR)=NPh] (R=Me, Et and iPr), upon in vitro cytotoxicity against the HT-29 colon cancer cell line and upon apoptotic pathways. *Journal of Inorganic Biochemistry*, *127*, 24–38. <https://doi.org/10.1016/j.jinorgbio.2013.05.011>
- Yoshida, S.-I., Kato, T., Sakurada, S., Kurono, C., Yang, J.-P., Matsui, N., ... Okamoto, T. (1999). Inhibition of IL-6 and IL-8 induction from cultured rheumatoid synovial fibroblasts by treatment with aurothioglucose. *International Immunology*, *11*(2), 151–158. <https://doi.org/10.1093/intimm/11.2.151>
- Zhang, C., Bourgeade Delmas, S., Fernández Álvarez, Á., Valentin, A., Hemmert, C., & Gornitzka, H. (2018). Synthesis, characterization, and antileishmanial activity of neutral N-heterocyclic carbenes gold(I) complexes. *European Journal of Medicinal Chemistry*, *143*, 1635–1643. <https://doi.org/10.1016/j.ejmech.2017.10.060>

**How to cite this article:** Espinosa AV, Costa DDS, Tunes LG, et al. Anticancer and antileishmanial in vitro activity of gold(I) complexes with 1,3,4-oxadiazole-2(3H)-thione ligands derived from  $\delta$ -D-gluconolactone. *Chem Biol Drug Des*. 2020;00:1–10. <https://doi.org/10.1111/cbdd.13757>